



ISSN: 2350-0328

**International Journal of Advanced Research in Science,  
Engineering and Technology**

**Vol. 4, Issue 2 , February 2017**

# **Theoretical issues in calculation of the impact Of a ball on a cylindrical surface**

**Fayzimatov Shuxrat Numanovich**

Ferghana Polytechnic Institute, 86, Ferghana street, 150100, Ferghana City, Republic of Uzbekistan.

**ABSTRACT:** The article focuses on the impact of aerodynamic flow on the free ball located inside the swirl chamber cavity. It analyzes the causes and magnitude of the forces acting on the free ball. Taking into account the forces of aerodynamic flow, particular attention should be paid to the intersection of solid mechanics and aerodynamics. Aerodynamic force acting on the ball is the input parameters for the equations of motion of a rigid body. This article is useful for a wide range of scholars in engineering and technical personnel involved in the automation of processes with cylindrical parts.

**KEY WORDS:** air stream, cylindrical surface, frequency

## **NOMENCLATURE**

$P$	power weight of sphere
$C_x$	coefficient resistance sphere
$r_{sph}$	radius sphere
$\rho_{str}$	density stream
$V_{rel}$	speed air relate to sphere
$V_{str}$	speed stream
$V_{sph}$	speed sphere
$V$	volume sphere
$g_{sph}$	specific gravity sphere
$m_{sph}$	sphere mass
$V_{sph}$	sphere speed
$\rho_{rot}$	sphere rotation radius
$R_{sph}$	sphere density
$\Gamma$	stream circulation
$\omega_{sph}$	circular speed sphere
$V_{rel}$	relative speed sphere
$r_0$	distance from the center sphere to rotation axis
$f_l$	coefficient of the nonsymmetrical distribution by the sphere surface
$K_{fr.rock}$	coefficient friction rocking

## **I. INTRODUCTION**

Existing methods and means of the surfactant treatment, a plastic deformation of internal surfaces of cylindrical parts, do not provide the increased production requirements because of low degree of mobility and it is difficult to automate. In order to receive work surface on the thin-walled cylindrical parts, by rolling-off with rotating ball, characterized by rigid contact with a working deforming element with the processing surface. A lack of rigid rolling is rather larger deformations

extending on all section of details that sometimes lead to axis curvature, change of geometry of details and non-uniform roughness of the processed surface.

Technological yield on manufacturing operations of thin-walled cylindrical parts is 60%. Thus the share of technological losses for semi-finished boring accounts about 19%, for fine-tuning the details with rolling-off rotating ball is 21%. These losses are caused by charging of a surface, changing of detail geometry and a non-uniform roughness of the processed surface. Moreover, experience shows that application of existing technology for viscous steels and alloys leads to sticking of the processed material on the work surface of rolling that reduces the quality of processing.

For specific dependencies, considering the influence of controllable factors on the speed of the ball and the force of its impact on the surface we will consider the interaction with the flow of the ball during the operation of the device. Considering that it is created the stable rotating stream in the device, let us consider the causes and magnitude of the force acting on the ball in more detail, placed in a vortex cavity of a chamber.

Taking into account that there is a stable rotation stream inside the device, careful measurements should be conducted on the quantity of power applied to the sphere inside vortex camera space.

The gas stream round the sphere may be divided into two components: axis  $\bar{F}_z$  along cylindrical pipe and circling around  $\bar{F}_\tau$ , used to tangent to the cylindrical pipe. Each of them acts to pipe differently. Axis component move the sphere along pipe's axis circle and makes the sphere rotate with frequency proportional to the stream speed and rotates around its own axis.

In simultaneous sphere rotation component of power  $\bar{F}_{cent}$  and carioles power  $\bar{F}_k$  works on it. Besides in Rota table stream with kauris decrease div pressure lie son the sphere and power  $\bar{F}_q$  works towards the vortex axis (Fig. 1, 2).

Result of these components  $\bar{F}_{ries}$  is held down the sphere with definite effort to cylindrical pipe's wall and calls reaction power in the places of contact. Concern of resultant component power's definition working on the sphere is complicated with the reason of that the stream is three dimensional, high speed and turbulent of stream.

Let's to see, when the power  $\bar{F}_{ries}$  excellent power of weight sphere and came up situation stability of equality. For this case to receive following permeation.

Current stream is stationary and submitting to Law Adiabatic  $P=\rho^k$ . The condition of income stream to cylindrical pipe non pay attention. The distribution of circular speed  $\bar{V}_\tau$  of stream describing on Law free whirlwind. Frequency circulation of sphere in cylindrical pipe is proportional to circular speed of stream, etc.  $f \sim \bar{V}_\tau$ .

As so above, take away power  $F_\mu$  influences on sphere from the side of stream can divided into two parts: axis and rounding. Axis consists of stream  $F_\mu \cdot \sin \alpha = P$ , where  $P$  – power weight of sphere. In general case, from the stream will influence power  $F_\mu$ , which equal [Ошибка! Источник ссылки не найден.1].

$$F_\mu = C_x \cdot \pi \cdot r_\omega^2 \frac{\rho_n \cdot V_{omh}^2}{2} \quad (1)$$

where  $C_x$  – coefficient resistance sphere;  
 $r_{sph}$  – radius sphere;  
 $\rho_{str}$  – density stream;  
 $V_{rel}$  – speed air relate to sphere.

According to the researches meaning  $C_x$  is changing in depending of character of stream. For our case selecting Numeral of Reynolds in  $R_e=10^3 \div 10^5$ . From the formula (1) to see that interaction stream with sphere the stream is feeling resistance its movement and following sphere moved with lagging behind from stream.

$$V_{rel} = V_{str} - V_{sph} \quad (2)$$

where  $V_{str}$  – speed stream;  $V_{sph}$  – speed sphere.  
 Besides power stream  $F_{\mu}$  on sphere will influence power weight sphere  $P$  which preventing its on moving through vertical and trend axis of cylinder.

$$P = V \cdot \gamma_{sph} \tag{3}$$

where  $V$  – volume sphere;  $\gamma_{sph}$  – specific gravity sphere.

However in future calculation can't to take into consideration influences power weight. We considered case stability of equal sphere in cylindrical pipe, where the axis consists of stream is  $F_{\mu} \cdot \sin \alpha = P$ .

Above mentioned under the influences of rounding consist power of stream  $\overline{F}_{\tau}$  sphere beginning circulation at rounding cylindrical pipe. According to mechanic during simultaneous rotation of sphere centrifugal and carioles power influences on it. In our case centrifugal power works on sphere with radius from rotation axis

$$F_{cent} = \frac{m_{sph} \cdot V_{sph}^2}{R_{rot}} = \frac{4}{3} \pi \cdot r_{sph}^3 \cdot \rho_{sph} \cdot \frac{V_{sph}^2}{R_{rot}} \tag{4}$$

where  $m_{sph}$  – sphere mass;  
 $V_{sph}$  – sphere speed;  
 $R_{rot}$  – sphere rotation radius;  
 $\rho_{sph}$  – sphere density.

Carioles power working on sphere is directed opposite to centrifugal hut action lines is matched. Carioles power is determined.

$$F_k = 2 \cdot m_{sph} \cdot \omega_{sph} \cdot V_{rel} \cdot \frac{1}{r_0}, \tag{5}$$

where  $\omega_{sph}$  – circular speed sphere;  
 $V_{rel}$  – relative speed sphere;  
 $r_0$  – distance from the center sphere to rotation axis.

As we know, during the rotated stream the statistic pressure lows and we get the four, which is directed to the sphere rotation axis. According [1] to its significance we get the formula.

$$F_g = f_1 \frac{\pi^2}{4} \rho_{str} \cdot \omega_{sph}^2 \cdot \frac{r_{sph}^2}{r_0}, \tag{6}$$

where  $f_1$  – coefricient of the nonsymmetrical distribution by the sphere surface.

But, above experimental researches show that according to calculation scheme, the action of this force is unimportant. Besides, the force Magnus will influence on the sphere.

$$F_{mag} = \rho_{str} \cdot V_{rot} \cdot \Gamma, \tag{7}$$

where  $\Gamma$  – stream circulation.

In the result of sphere interaction with cylindrical pipe in place them contact appeared power reaction  $N$  which acting tangent to surface pipe in a direction to the centre of sphere and power of friction  $F_{fr}$  on a directed opposite movement

sphere. On the place of contact sphere with cylindrical pipe is acting moments of friction rocking. On the Fig. 1 is shown scheme of power on the place of contact sphere with cylindrical pipe on a plane perpendicularly axis pipe. According to Fig. 1

$$\begin{aligned} F_{fr} &= N \cdot K_{fr.rock} \\ M_{fr} &= N \cdot K_{fr.rock} \end{aligned} \tag{8}$$

where  $K_{fr.rock}$  – coefficient friction rocking.

Definition power which acting to sphere is shown schematically in the moment of contact sphere with cylindrical pipe (Fig. 2) On a bases of analyses receiving making equalization power on the sphere for case equality rounding by projection all powers into axis  $X$  and  $Y$ .

In general case equalization of projection power axis coordination can be written in this way:

$$\begin{aligned} \sum F_x &= 0, & \sum F_y &= 0, & F_{fr} &= F_{\mu} \\ N &= F_c - F_k - F_{mag} - F_q, & & & & \\ N &= F_{ries} & & & & \\ \sum M &= 0, & F_{\mu} \cdot r_{sph} &= N \cdot K_{fr} \end{aligned} \tag{9}$$

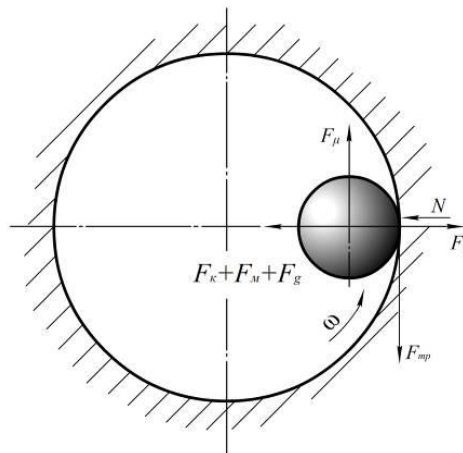


Fig. 1 The scheme of force in points of sphere contact with cylindrical pipe.

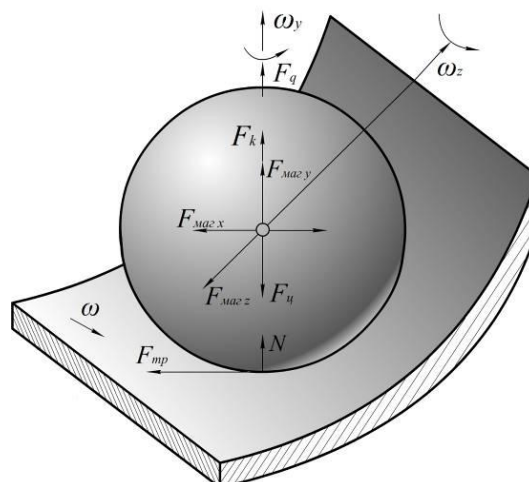


Fig. 2 The general scheme of force

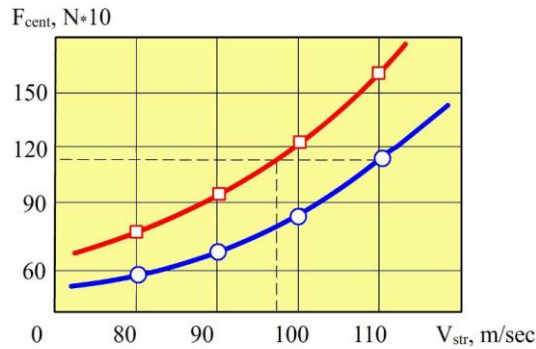


Fig. 3 Depend of the speed sphere  $V_{sph}$  inversely the speed stream  
 $\square$  – when  $R=30$  mm;  
 $\circ$  – when  $R= 14,5$  mm.

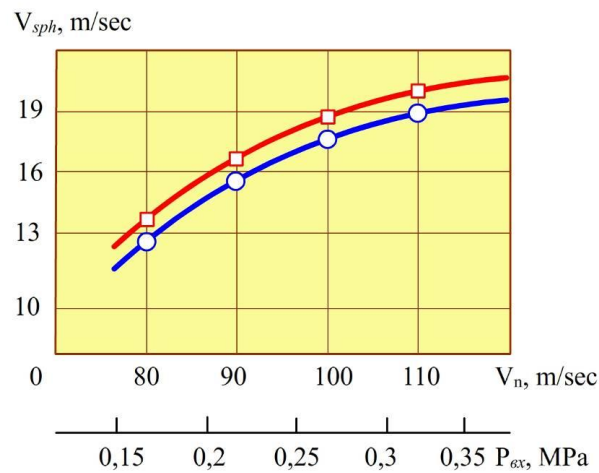


Fig. 4 The impact of speed stream on centrifugal force of putting sphere to the surface.  
 $\square$  – when  $R=30$  mm;  
 $\circ$  – when  $R= 14,5$  mm

If we place the received formulas for the force in the equation (9) we get:

$$C_x \cdot \pi \cdot r_{sph}^2 \frac{\rho_{str} \cdot V_{rel}^2}{2} \cdot r_{sph} = \frac{m \cdot V_{sph}^2}{R_{circ}} \cdot K_{fr} \quad (10)$$

Having known, that  $V_{rot} = V_{str} - V_{sph}$  after simple transformations, determine the sphere speed.

$$V_{sph} = \frac{V_{rel}}{1 + \sqrt{\frac{2mK_{fr,rock}}{C_x \pi \cdot r_{sph}^3 \cdot \rho_{rel} \cdot R_{circ}}}}, \quad (11)$$

The equation (11) shows, that before even sphere rotation it fails from the stream on the quantity.

$$1 + \sqrt{\frac{2mK_{fr.rock}}{C_x \pi \cdot r_{sph}^3 \cdot \rho_{rel} \cdot R_{circ}}}$$

The getting expression (11) allows us to determine how the sphere influence on the putting sphere.

$$F_{ries} = \frac{m_{sph} \cdot V_{sph}^2}{R_{circ}} = \frac{m \cdot V_{str}^2}{R_{circ}} \left( 1 + \sqrt{\frac{2mK_{fr.rock}}{C_x \pi \cdot r_{sph}^3 \cdot \rho_{str} \cdot R_{circ}}} \right)^{-2} \quad (12)$$

At the Fig. 3. the calculation significances of the speed sphere  $V_{sph}$  inversely the speed stream  $V_n$  for the compass of ration of the diameters sphere and working details  $D_1$ .

$$\frac{d_{sph}}{D_1} = 0,65 \div 0,08. \quad (13)$$

The analysis of the getting results shows that with increasing of speed of sphere moving along the working surface, which leads to the growth of centrifugal force of putting sphere to the surface.

To provide the conditions under which the deformation occurs of the surface layer, it is necessary to determine the contact stresses that occur during contact with the ball surface being treated. To do this, knowing the centrifugal force of compression of the ball to the surface and using the formula of Hertz [2], we can estimate the contact stress arising from the interaction sphere with the surface being treated.

At the same time to simplify the problem, we make the following assumptions:

- absolutely smooth surface feel and unpolluted;
- neglect axial movement relative to the surface.

Solving the problem under the above assumptions, we will try to correct the results, taking into account the above factors and the experimental data. Analysis (12) shows that for the case when a sphere of radius  $R_{sph}$  in contact with a cylindrical cavity of radius  $R$ , coefficient of rolling friction depends on the diameter of the ball, the ball diameter ratio to the radius of the work piece, the elastic modulus contacts are the bodies of efforts, as well as the magnitude of the microscopic irregularities of the surface layer. According to the mentioned above assumptions, the coefficient of rolling friction (Fig. 16) for the ideal case is  $K_{fr} = K$  (13) where the value of the circular contact area,  $K$  - coefficient taking into account the position of the resultant pressure forces the ball at the site of contact ( $0 < K < 1$ ). The value of the radius of circular contact area, according to [3] is defined:

$$a = 0,9086 \sqrt[3]{\eta \cdot F_{uz} \cdot r_n}, \quad (14)$$

where  $r_n$  - reduced radius of the sphere and cylinder at the point of contact, which is equal  $r_n = \frac{R \cdot r}{R - r}$ .  $F_{uz}$  - centrifugal force of compression of the ball to the surface;  $\eta$  - elastic constant of the contacting bodies, which is equal

$$\eta = \frac{1 - \nu_1^2}{E_1} + \frac{1 - \nu_2^2}{E_2}. \quad (15)$$

Here  $\nu_1, \nu_2$ , and  $E_1, E_2$  - respectively the Poisson's ratios and elastic moduli of the sphere and cylinder. The value of the contact stresses between the contacting bodies, according to [3] can be written as:

$$\sigma = 0,5784 \sqrt[3]{\frac{F_{uz}}{\eta^2 \cdot r_n^2}} \quad (16)$$

or

$$F_u = \frac{\sigma^3 \cdot \eta^2 \cdot r_n^2}{(0,5784)^3}$$

Substituting (16) (14), we find the radius of the circular contact area

$$a = 0,9086 \sqrt{\frac{\sigma^3 \cdot \eta^2 \cdot r_n^2}{(0,5784)^3}} \cdot \eta \cdot r_n = 1,571 \cdot \sigma \cdot \eta \cdot r_n, \quad (17)$$

In general, equation (12), in light of the above relationships can be written as follows:

$$\frac{\sigma^3 \cdot \eta^2 \cdot r_n^2}{(0,5784)^3} = \frac{m \cdot V_n^2}{R \cdot \sqrt{\left(1 + \frac{2mK_{mp.kau}}{C_x \pi \cdot r_{uu}^3 \cdot \rho_n \cdot R_{gp}}\right)^2}} \quad (18)$$

Substituting the value of the coefficient of rolling friction in (18), after simple transformations, we obtain the dependence that allows determining the contact stresses arising from the interaction with the ball on the surface:

$$\sigma^3 = \frac{6318 \cdot V_n^2 \cdot r_{uu}^3}{\eta^2 \cdot r_n^2 \cdot R \cdot \left(1 + \sqrt{58190 \frac{K}{R} \sqrt{1,234 \sigma \cdot \eta \cdot r_n^2}}\right)^2} \quad (19)$$

The solution of equation (19) with the use of computers was performed at following parameters: the radius of the steel ball  $r = 0,5 \div 3,0$  mm, with a modulus of elasticity  $E = 2 \cdot 10^{11}$  Pa, Poisson's ratio  $\nu = 0,3$  in contact with the cylinder  $R = 10, 15, 20$  mm,  $E = 0,71 \cdot 10^{11}$  Pa,  $\nu = 0,3$ . Analysis of the results shows that the allowable stresses in the process of contact with the surface of the ball, much higher than the yield stress of the workpiece, ie,  $\sigma_d \gg \sigma_t$ . This is due to the fact that the surface we assumed perfectly smooth and uncontaminated. For small size of the contact boundary of the flow of the material are so small that they violated the dislocation mechanism of plastic deformation. This increases material yield and, consequently, the contact stress at the contact. Furthermore, the high velocity of the ball on the surface causes the momentary contact with the surface of the ball and can not develop the process flow. Thus, there is over-voltage of the surface layer.

It should also be noted that the yield strength of the material during processing increases due to strain hardening. This increase is caused by a high speed of moving ball along the work piece and the presence of the ball micro impacts over surface arising from the heterogeneity of the surface layer turbulence and vortex.

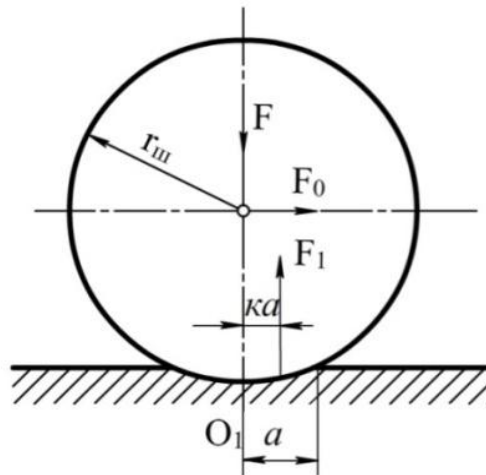


Fig. 5 Scheme of the contact protrusions of the defect layer with a ball (for the ideal case)

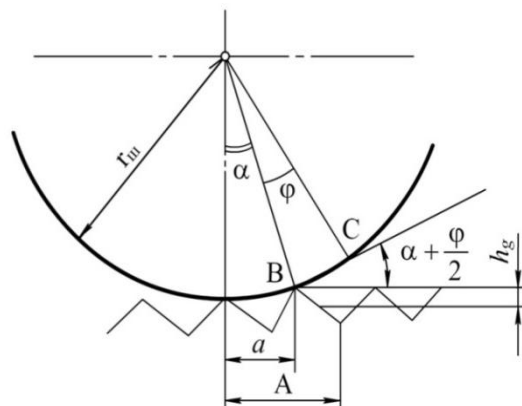


Fig. 6 Scheme of the contact protrusions of the defect layer with a ball (with defected layer.)

The magnitude of contact stress during plastic deformation in real terms significantly affected by the presence of the defect layer (roughness, contamination of oxide films, etc.). In this case the top of asperities are located on different levels and the emergence of zones of plastic deformation does not occur simultaneously in all the contact points. Consider the case of interaction with the surface of the ball based on the availability of the defect layer, closer to real conditions.

Figure 6 b shows a diagram of the formation of asperities contact protrusions with the ball. In reality, due to the presence of dirt and asperities coefficient of rolling friction is much higher than in the ideal case. According to Figure 6, b coefficient of rolling friction is:

$$\kappa_{Tp} = K \cdot A \tag{20}$$

where K - coefficient taking into account the position of the resultant pressure forces the ball at the site of contact, A - the value of the contact area, taking into account the defect layer, which is equal in our case  $A = R \cdot \sin(\alpha + \varphi)$  or the smallness of  $\alpha + \varphi$ .

$$A = R(\alpha + \varphi). \tag{21}$$

From the triangle we find



$$\varphi = \frac{K}{r},$$

where

$$K = \frac{h}{\sin\left(\alpha + \frac{\varphi}{2}\right)} = \frac{h}{\alpha + \frac{\varphi}{2}},$$

In this case h – height of the defect layer, which is equal

$$h = h_3 + h_M,$$

where  $h_3$  – height of polluted layer:  $h_M$  – height of asperities. Subsequently:

$$\varphi = \frac{h}{\left(\alpha + \frac{\varphi}{2}\right) \cdot r_n}$$

where  $r_n$  - radius of the ball. After simple transformations we obtain

$$\varphi = \sqrt{\alpha^2 + \frac{2h}{r_n}} - \alpha, \tag{22}$$

We assume (22) in (21) and acknowledging that  $\alpha = \frac{a}{2}$ , we find the value of the contact area, taking into account the defect layer:

$$A = \sqrt{a^2 + 2hr}, \tag{23}$$

where h – height of polluted layer; a – magnitude of the circular contact area.

Assuming (23) in (20), we obtain the value of the coefficient of rolling friction in the light pollution and asperities

$$K_{mp} = K \sqrt{a^2 + 2hr_n}, \tag{24}$$

With (24) (19) for a real case can be written as:

$$\sigma^3 = \frac{6318 \cdot V_n^2 \cdot r_u^3}{\eta^2 r_n^2 R \cdot \left(1 + \sqrt{58190 \frac{K}{R} \sqrt{1,234 \sigma^2 \eta^2 r_n^2 + h \cdot r_n}}\right)^2} \cdot \tag{25}$$

In  $h \geq 1,0$  mk this can be expressed as:

$$\sigma^3 = \frac{6318 \cdot V_n^2 \cdot r_u^3}{\eta^2 r_n^2 R \cdot \left(1 + \sqrt{58190 \frac{K}{R} \sqrt{h \cdot r_n}}\right)^2}$$

Or in  $r < R$  (more than 10 times)

$$\sigma^3 = \frac{6318 \cdot V_n^2 \cdot r_{in}}{\eta^2 \cdot R \cdot \left(1 + \sqrt{58190 \frac{K}{R} \sqrt{h \cdot r_n}}\right)^2} \quad (26)$$

The solution of equation (25) with the use of computers made in the following blowing within the parameters: h - 0.2 microns to 10 microns; Rsh - from 0.5 mm to 3.0 mm. R-value to be equal to 10, 15, 20 mm.

Calculations were performed for a steel ball E = 2 • 1011 Pa, ν = 0,3 and for a cylinder made of aluminum E = 0,71 • 1011 Pa, ν = 0,3.

The influence of the radius of the contact stress at the flow rate Vp = 90 m / sec, the radius of Workpiece R = 20 mm and different values of the defect layer h are given in Figure 7.

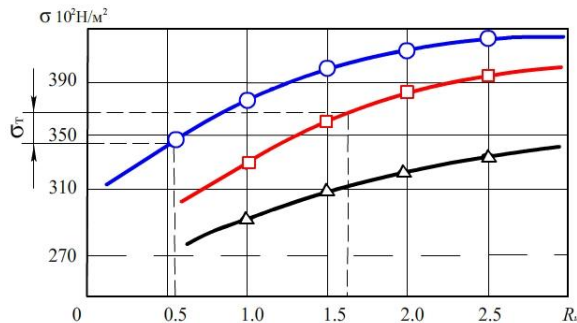


Fig. 7 The influence of the radius on the contact stress at Vp = 90 m / sec, R = 20 mm.

- - when h=2,5 mm;
- - when h=5,0 mm;
- △ - when h=10 mm.

As can be seen from the graphs (Fig. 7), with an increase in the radius to Rsh = 2.5 mm distorting its action increases and, consequently, increased contact stresses. With the increase of the same height h of the defect layer contact stresses are reduced (Fig. 8). This is because the presence of contaminants on the surface of the work piece, as well as condensation of water vapor in the air create ledges asperities film layer that prevents the convergence of their contacts are tel.

As follows from (25), the main parameter influencing the magnitude of the contact stress is the flow velocity vn. Fig.8 shows the dependence of contact pressure on the flow velocity at Rsh = 1.0 mm.

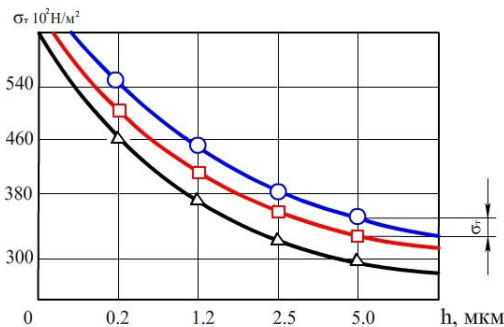


Fig. 8 Effect of defect layer on the contact stress at r<sub>in</sub> = 1,0mm.

- - when V<sub>n</sub>=100 m/sec;
- - when V<sub>n</sub>=90 m/sec;
- △ - when V<sub>n</sub>=80 m/sec.

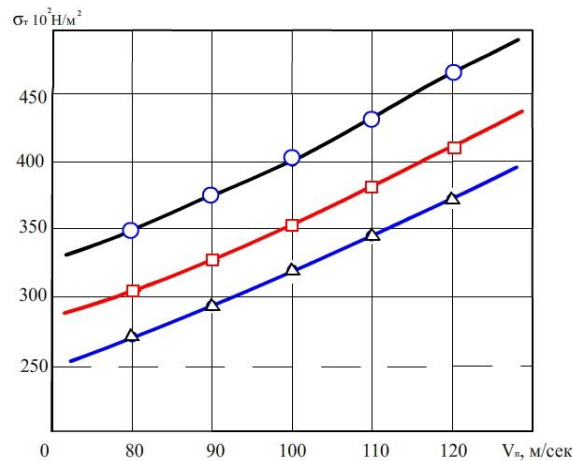


Fig. 9 The dependence of the contact stress on the flow rate at  $r_{III} = 1,0$  mm.

- $\bigcirc$  - when  $h=10$  mm;
- $\square$  - when  $h=5,0$  mm;
- $\triangle$  - when  $h=2,5$  mm.

Fig. 9 shows that the contact stress increases with increasing flow rate. This result is logical, because the increase in flow rate leads to an increase in the speed of the ball and therefore the centrifugal force compression of the ball to the surface (see Fig. 6). Another parameter that affects the value of contact stress, is the radius of the work piece (Fig. 9).

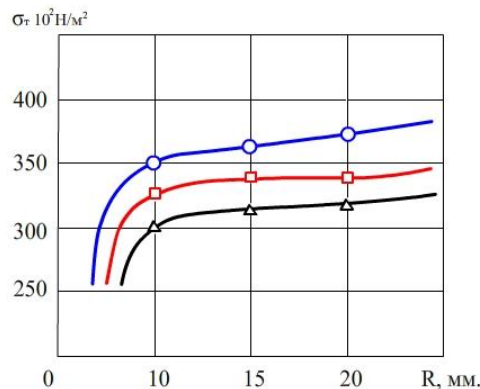


Fig. 10 The dependence of the contact stress on the radius of the workpiece at  $r_{III} = 1,0$  mm,  $h=5$  mm.

- $\bigcirc$  - when  $Vn=100$  m/sec;
- $\square$  - when  $Vn=90$  m/sec;
- $\triangle$  - when  $Vn=80$  m/sec.

The results show that the change in the range of  $p_a \rightarrow$  radius of the work piece 10 to 20 mm, the contact stresses vary slightly. Analysis of the results obtained above allow us to choose a first approximation, the radius of the ball and the flow rate depending on the physical and mechanical properties of the work piece and the initial state of the surface layer. The optimal value of the radius to the above case, according to the results lies within  $R_{sh} = 1,0 \div 2,5$  mm. Given that the turnover of the work piece occurs when  $\sigma_t = (340 \div 360) 10^6$  H/m<sup>2</sup>, and in real value of the defective parts of the layer under study is in the range  $h = 5,0 \div 10$  mm, the flow rate is chosen in the range of  $V_p = 90 \div 100$  m/sec (Fig. 9).



ISSN: 2350-0328

# International Journal of Advanced Research in Science, Engineering and Technology

Vol. 4, Issue 2 , February 2017

Thus, the above theoretical relationships, allow us to estimate the impact force of the ball on the surface and determine the contact stresses in interaction with the surface of the ball. This allows a first approximation to select mode parameters finishing and hardening treatment, depending on the yield strength of the material and the initial state of the surface layer of the work piece.

## II. CONCLUSION

There is particular issue in considering aerodynamic forces and flow acting on the ball, that is located at the intersection of solid mechanics and aerodynamics. Because of heterogeneity and nonstationarity of aerodynamic flow and the presence of asperities treated surface appears a series of blows on the surface of the ball and accurate quantitative theory describing the processes of such strikes do not currently exist.

Theoretical description of the interaction of aerodynamic flows with a free ball at the given parameters of the device is only possible if the force  $F_{res}$  greater than the force of weight of the ball and there is a situation of stable equilibrium.

The yield stress of the material increases as a result of hardening condition. This increase is caused by movement of the ball at high speed along the work surface and the presence of the balls impact over the surface that arises from the heterogeneity of the surface layer turbulence and aerodynamic flow.

The magnitude of contact stress during plastic deformation in real terms significantly affected by the presence of the defect layer (roughness, contamination of oxide films, etc.). In this case the top of asperities are placed at different levels and the emergence of zones of plastic deformation does not occur simultaneously in every contact points.

## REFERENCES

1. Шонин А.Н., Комаров Ю.А., Коноплев Ю.С. Методика расчета скоростных расходомеров со свободновращающимся шариком, НИИ теплоприбора, 1965, № 4, [Shonin A.N., Komarov Yu.A. Konoplev Yu.S. (1965) Method of calculation of speed measure with free rotation of a small ball. SRI Teplopribor, No 4.]
2. Меркулов А.П. Вихревой эффект и его применение в технике. Самара: Оптима, 1997. [Merkulov, AP (1997) Vortex effect and its applications in engineering. Samara: Optima,.]
3. Кузнецов В.И., Барсуков С.И. Вихревой эффект Ранка : монография / – Иркутск: Изд-во Иркут. ун-та, 1983. [Kuznetsov VI, Barsukov, S. (1983) Vortex Ranque: monograph. Irkutsk: Irkut Press.]